# Phenotypic plasticity facilitates alterations in life-history strategies under combinations of environmental stresses

Lidor Shaar-Moshe[1], Ruchama Hayouka[1], Ute Roessner[2] and Zvi Peleg[1*]

[1.] The Robert H. Smith Institute of Plant Sciences and Genetics in Agriculture, The Hebrew University of Jerusalem, Rehovot 7610001, Israel.

[2.] School of BioSciences, The University of Melbourne, Melbourne 3010, Australia.

**Author for correspondence**: Zvi Peleg

Tel: +972-8-9489638

Email: zvi.peleg@mail.huji.ac.il

**Summary**

- Plants developed various reversible and non-reversible acclimation mechanisms to cope with the multifaceted nature of abiotic stress combinations. We hypothesized that in order to endure different combinations of stresses, plants elicit unique acclimation strategies through specific alterations of their energy balance.
- A system biology approach, integrating physiological, metabolic and transcriptional data, was applied to investigate *Brachypodium distachyon* acclimation strategies to double and triple stress combinations of salinity, drought and heat. In addition, the various trade-offs between functional and performance traits and their effects on plant fitness were analyzed.
- We found that under combination of stresses plants exhibited phenotypic and metabolic plasticity that differentially affected plant life-history strategy. Combination of drought and heat resulted in escape strategy, while under combination of salinity and heat plants exhibited avoidance strategy. On the other hand, under combinations of salinity and drought, with or without heat, plant fitness was severely impaired.
- Under the combined stresses, plant life-history strategies were shaped by trades-off between traits and the limits of phenotypic and metabolic plasticity. This study shed light on unique acclimation mechanisms that can contribute to grass fitness and possibly to their dispersion under changing environments.

**Key words**: Abiotic stress combinations, fitness, gene expression, life-history strategy, metabolomics, physiology, stress acclimation, trade-off.

# Introduction

Phenotypic plasticity, the ability of a given genotype to express different phenotypes under alternative environmental conditions (Pigliucci, 2001), is a fundamental feature of plants, enabling them to optimize their fitness under changing and uncertain environments (Matesanz *et al.*, 2010). The capacity of an organism to express plasticity in a given trait is mediated at the molecular level (Schlichting & Smith, 2002) and involves various reversible and non-reversible developmental, anatomical, morphological and physiological modifications (Nilson & Assmann, 2010). In contrast to genetic alterations that occur across several generations, phenotypic plasticity accounts for the plant responses to environmental changes within the life span of an individual plant (Bradshaw, 1965). It is assumed that the ability of phenotypic plasticity to alleviate short-term environmental changes, could also be beneficial upon the long-term effects of climatic changes (Jump & Peñuelas, 2005). These changes are predicted to alter plant growth, reproduction and survival, the main traits of life-history, which aims at understanding and predicting the existence of plants with different traits and strategies (Grime, 1977). The three performance traits, which directly contributing to plant fitness, can be modulated by morphological, physiological or phenological traits (i.e. functional traits) (Violle *et al.*, 2007).

Plant life-history strategies rely on trade-offs in resource partitioning between growth, reproduction and defense, due to resource limitations, and/or environmental stresses (Bazzaz *et al.*, 1987). These constrains limit the capacity of the plants to acquire net carbon and alter the energy balance and allocation of assimilates from growth and reproduction into defense (Sultan, 2000). Variations in life-history strategies usually involve cross-species comparisons (e.g. (Salguero-Gomez *et al.*, 2016). However, owing to their phenotypic plasticity, plants from the same genotype growing in different environments, can differ in the trade-offs of resource allocation, thus, exhibiting different life-history strategies (De Deyn, 2017). One of the challenges of plant biology is to identify these genetic trade-offs and through a mechanistic understanding manipulate them for crop improvement (Des Marais & Juenger, 2016).

Environmental stresses, such as soil salinization, drought episodes and heat waves, are among the main factors limiting plant performance and affecting their ecological fitness. At the Mediterranean-like conditions, these stresses usually occur simultaneously, effecting both natural and agricultural systems (Vautard *et al.*, 2007; Maggio *et al.*, 2011). Moreover, based on climate change models, plants are projected to encounter a greater range and number of abiotic stress

combinations in the near future (Mittler & Blumwald, 2010). To cope with such environmental constrains, plants have evolved a variety of acclimation mechanisms. These mechanisms can be encapsulated to two main strategies: *escape* (e.g. rapid completion of plant life cycle or deeper rooting), and *resistance*, which is sub-divided to *avoidance* (altering or halting the effect of the stress through mainly morphological and/or anatomical changes), and *tolerance* (maintaining normal functions despite the presence of the stress through molecular mechanisms) (Levitt, 1972; Mickelbart *et al.*, 2015). Plants can combine acclimation mechanisms from different strategies, thus eliciting an environmentally induced phenotypic variation.

*Brachypodium distachyon* (L.) Beauv. is a model system for Pooid cereal and forage species that has been used to study environmental stress responses such as: drought, extreme temperature, salinity and oxidative stress (e.g. (Priest *et al.*, 2014; Shaar-Moshe *et al.*, 2015; Cao *et al.*, 2016; Bian *et al.*, 2017; Wen *et al.*, 2017). However, except for a few studies (e.g. (Barhoumi *et al.*, 2010; Des Marais *et al.*, 2017; Shaar-Moshe *et al.*, 2017), most of these experiments involved single stresses at early vegetative stages. In order to study *B. distachyon* acclimation strategies to environmental stresses, information on life-history and phenological data is required since they determine the coordination of environmental conditions with developmental transitions, the occurrence of the stress and the expected acclimation strategy (Des Marais & Juenger, 2016).

Recently we have shown a unique transcriptional signature among genes that were expressed only under combinations of stresses. This transcriptional pattern was enriched with antagonistic responses, which suggested an alteration in the mode of action under combined stresses (Shaar-Moshe *et al.*, 2017). Here we used system biology approach to test two hypotheses: that plant energy balance was differentially impaired in each combination of stresses, and that plants elicited a unique acclimation strategy, with distinct trade-offs in life-history traits of growth, reproduction and defense, under each combination. The aims of the current study were to ***i***) quantify the effects of combined stresses on plant fitness and its associated performance traits, ***ii***) characterize the effects of combined stress on the photosynthesis apparatus and energy metabolism, and ***iii***) identify trade-offs between functional and performance traits within the combined stresses. Our results provide a mechanistic understanding of plant acclimations to combinations of stresses and shed light on the unique strategies plant employed under different environmental constrains.

# Materials and Methods

## Plant material and growth conditions

*Brachypodium distachyon* accession *Bd*21-3 plants were grown as previously described (Shaar-Moshe *et al.*, 2017). Briefly, following 48h at 4ºC to synchronize germination and 5d at 15ºC to establish germination, uniform seedlings were transplanted into pre-weighted 1L pots and transfer to a Phytotron (22ºC day/ 16ºC night, 10h light / 14h dark). The dry and fully irrigated weight of the pots were used to calculate soil water content (SWC). Plants were irrigated to runoff with fresh water three times a week, and fertilized with 1 g $L^{-1}$ N:P:K (20% nitrogen, 20% phosphorus and 20% potassium) + micronutrients, eight weeks after germination. Ten weeks after germination, plants transferred to a long day regime (15h light/ 9h dark).

Each plant was subjected to one of the following five treatments in a split-plot factorial (treatment) complete random design: *Control* (***C***), plants were grown at 22ºC day/ 16ºC night throughout the experiment. Combination of salinity and heat (***S&H***), plants were exposed progressively to salinity, starting at five-leaf stage, by two irrigations of 20mM NaCl, followed by five irrigations with 50 and then 80 mM NaCl. Target concentration of 100 mM NaCl, which was achieved within four weeks, was kept throughout the experiment. Runoff electric conductivity was monitored weekly. At anthesis, plants were transferred on 20:00 pm, to a pre-heated greenhouse at the Phytotron (34ºC day / 28ºC night) for four days. Combination of drought and heat (***D&H***), plants were gradually exposed to water stress, starting at booting stage (BBCH scale 45; Hong *et al.*, 2011, approximately 12 weeks after germination), by withholding irrigation. Each pot was weighted every second day and relative soil water content was maintained at 40% for 17 days. At anthesis, plants were subjected to heat stress as described above. Combinations of Salinity and drought (***S&D***) and (***S&D&H***), stresses were applied as described above. Under these combinations, plants were irrigated with fresh water once drought stress was imposed.

**Performance traits and plant fitness**

Plants were documented and measured for shoot dry weight (DW) at three developmental stages: 4 days after anthesis (DAA), 12 DAA and 17 DAA; *n*=3). At the end of the growing season, when plants from all treatments senesced, spikes and shoots, from each plant, were separately harvested (*n*=5) and oven-dried (75°C for 96h). Samples were weighted to determine shoot DW. The reproductive samples were threshed and grain were weighted and counted to obtain 100-grain weight. The ratio between spike DW (i.e. reproductive output) and whole shoot DW was used to calculate the reproductive allocation. Grain parameters were analyzed using GrainScan software (Whan *et al.*, 2014). Germination assay was performed using the "cigar roll" method (Watt *et al.*, 2013). Twenty uniform grains, which developed on plants subjected to control or stress combination treatments (*n*=3), were placed on a moist germination paper (25 × 38 cm; Anchor Paper Co., St. Paul, MN, USA), three cm from the top of the sheet, with the embryo facing down. The paper was covered with additional sheet of moist germination paper and then rolled tightly to a final diameter of ~4 cm. The base of the rolls was dipped in a tray of tap water and stored in darkness for 48h at 4°C, followed by 6d at 15°C for establishment of germination. The number of grains with the primary seminal root was recorded to determine grain viability.

**Functional traits**

Measurements of chlorophyll fluorescence and content were conducted in a complete random design at three developmental stages: 4 DAA, 12 DAA and 17 DAA, on the mid portion of the adaxial side of the third leaf. Chlorophyll fluorescence was measured using a portable chlorophyll fluorometer MINI-PAM-II (Walz GmbH, Effeltrich, Germany). Dark-adapted $Fv/Fm$ was determined following 40 min of whole plant dark-adaptation (*n*=4). $Fv/Fm$ values that represent maximal photochemical efficiency of photosystem II were automatically calculated as $(Fm-F_0)/Fm$ by the WinControl-3 software. Chlorophyll content (SPAD value; *n*=4) was assessed by the SPAD-502 chlorophyll meter (Minolta Camera Co., Japan). Each SPAD value is the mean of five technical replicates measured from five different leaves, per plant. Carotenoid content and plant senescence were estimated using none-distractive reflectance measurements, on the mid portion of the adaxial side of the third leaf, by the CI-710 Miniature Leaf Spectrometer (CID Bio-Science, USA), at 4 DAA. Integration time was 800 milliseconds, boxcar width was 10 points and each value represents an average of four scans. The following reflectance indices were used for

carotenoid fluorescence: $CRI_{550} = (1/W_{510})-(1/W_{550})$ (Gitelson *et al.*, 2002) and plant senescence: $PSRI=(W_{680}-W_{500})/W_{750}$) (Merzlyak *et al.*, 1999). The level of total reactive oxygen species (ROS) was determined with 2′,7′-dichlorofluorescin diacetate ($H_2$DCFDA; Sigma) fluorescence dye as described in (Jang *et al.*, 2012),with minor modifications. At 4 DAA, leaf discs (0.5 mm diameter), were samples from the mid portion of the third leaf, and placed in 96 well plates containing 10 mM Tris-HCl pH 7.5. Each leaf was sampled twice and the matching samples were allocated to two identical sets, each containing three technical repeats (i.e. three leaves per plant) from each treatment (*n*=4). Subsequently, leaf discs from one set were transferred to a new 96 well plate containing 50 µM $H_2$DCFDA, in 10 mM Tris-HCl pH 7.5, for 60 min. The other set served as control and was used to subtract background signal. Fluorescence measurements were conducted by a Tecan Infinity 200PRO multi-well plate reader (Tecan Ltd., Switzerland) on the adaxial side of the leaf discs, with excitation at 485nm and emission at 535nm. Gain was manually set to 41 and each value is the mean of 25 flashes. Measurements of relative water content (RWC) and osmotic adjustment (OA) were performed on the third leaves at mid-day (*n*=5), as described previously (Shaar-Moshe *et al.*, 2015). Ion concentrations (i.e. $Cl^-$, $Na^+$ and $K^+$), under control and stress treatments, were evaluated based on (Yermiyahu *et al.*, 2017). Oven-dried leaf samples (*n*=6) (75°C for 96h) were ground to a fine powder. One hundred mg from each sample was added to 10 mL double-distilled water (DDW), followed by an overnight incubation. Sodium and potassium concentrations were analyzed by atomic absorption (PerkinElmer Precisely Analyst 200) and chloride concentrations were quantified with chloridometer (MK II Chloride Analyzer 926, Sherwood Scientific Ltd., Cambridge, UK).

**Transcriptional data and analysis**

Extraction of RNA from flag and second leaf samples, preparation of cDNA libraries and their sequencing as well as data processing, analysis of differentially expressed genes and their annotation were obtained form (Shaar-Moshe *et al.*, 2017). Files of the raw mRNA-seq are available at the short-read archive of the National Center for Biotechnology Information (https://www.ncbi.nlm.nih.gov/sra) under accession number PRJNA360513.

**Determination of starch content**

Starch content was determined as described previously (Naschitz *et al.*, 2010), with minor modifications. Briefly, 50 mg of lyophilized leaf samples (*n*=5) that were collected at 5 DAA at 18:00 pm were ground with liquid nitrogen and rinsed three times with 80% ethanol to remove soluble sugars. The pellet was fluidized with DDW and starch was hydrolyzed with amyloglucosidase (Sigma), in 15 mM sodium acetate pH 4.5, overnight at 55°C. Subsequently, soluble sugar content was determined spectrophotometrically with Epoch plate reader, with absorbance at 340 nm, using Glucose (HK) assay kit (Sigma).

**Metabolite extraction**

Flag and second leaf (*n*=5) were harvested at 4 DAA, immediately frozen in liquid nitrogen and stored at -80°C until lyophilization. Accurate sample weight was recorded and samples were transferred to cryo-mill tubes (Precellys 24, Bertin Technologies). Methanol (MeOH, 500 µL) containing the internal standards [D-Sorbitol-$^{13}C_6$ (0.02 mg/mL) and L-Valine- $^{13}C_5$,$^{15}N$ (0.02 mg/mL), Sigma Aldrich (Australia)] was added to the samples, followed by vortex and homogenization (3 × 45 s at 6400 rpm) at −10°C using a Cryomill (Precellys 24, Bertin Technologies). The samples were then extracted at 70°C in a thermomixer at 850 rpm, and centrifuged for 5 min at 4°C, at 13,000 rpm. The MeOH supernatant was collected into new reaction tubes and 500 µL water (Milli Q grade) was added to the tubes containing the sample pellet, followed by vortex-mixed for 30 s, and centrifuged at 13,000 rpm for 10 min at 4°C. The supernatants were combined and 100 µL were dried *in vacuo* for gas chromatography–mass spectrometry (GC–MS) untargeted analysis.

**Derivatization for GC–MS analysis**

Derivatization for GC–MS analysis was carried out as described in (Dias *et al.*, 2015). After completion of derivatization, samples were set for one hour and then 1 µL was injected onto the GC column using a hot needle technique. Splitless and split (1:20) injections were performed for each sample.

## Untargeted GC–MS and statistical analysis

Untargeted GC–MS analysis and data analysis were carried out as described in (Hill *et al.*, 2015). The metabolite data were analyzed with the open-source software, MetaboAnalyst 3.0 (Xia & Wishart, 2016). Interquartile range was used for data filtering, followed by log transformation for data normalization. The metabolites are presented as fold change (FC) values relative to control conditions and a 10% false discovery rate correction for multiple comparisons (Benjamini & Hochberg, 1995), was used to detect significant alterations in metabolite accumulation.

## Statistical and data analyses

Measurements of functional and performances traits, as well as correlation between gene expression data and functional traits or metabolites were analyzed statistically using JMP® pro 13 statistical package (SAS Institute, Cary, NC, USA). All traits were examined for homoscedasticity among treatments. Differences between control and stress treatments, were detected using one-way analysis of variance (ANOVA), followed by Dunnet's test at $P \leq 0.05$. In the absence of homoscedasticity among treatments, nonparametric comparisons with Steel method ($P \leq 0.05$) were used to detect differences between control and stress conditions. Differences between two treatments were detected using Student's *t*-test at $P \leq 0.05$. Principle component analysis (PCA), based on $\log_2$ fold change (FC) values of genes assigned to functional categories (e.g. carotenoid synthesis and starch metabolism), was used to identify the first principal component (PC1, eigenvalues > 1) that accounted for the maximal variation among gene expression. Associations between PC1 and the FC values of the corresponding functional traits or metabolites were studied using Pearson correlation analysis at $P \leq 0.1$. In the lack of liner relationship, nonparametric correlation with Spearman's correlation was used. Correlations between traits or between metabolites were studied using Pearson correlation analysis at $P \leq 0.05$. PCA was used to evaluate the association between osmolytes (i.e. 11 metabolites and three ions) and OA and RWC. PCA is presented as a biplot of the two major PCs (Eigenvalues > 1). Line and box plots were generated by ggplot function in ggplot2 package.

# Results

## Under S&H plants maintained their reproductive allocation, while under S&D and S&D&H their fitness was severely impaired

In general, all stress combinations resulted in detrimental phenotypic effects, including an overall reduction in plant height and biomass, as well as a decline in chlorophyll content (SPAD units; Fig. 1a). Yet, depending on the stress combination, plants elicited a differential acclimation response that varied in its magnitude and timing. For example, under drought and heat (D&H), chlorophyll content decreased by 20% and 82%, at 4 DAA and 12 DAA (i.e. at grain filling), respectively, yet all other stress combinations resulted in significant reductions, below control levels, only at 17 DAA (during grain maturation period) (Fig. 1b, Table S1). Genes involved in chlorophyll degradation were generally up-regulated under combined stresses, mainly under D&H. This stress combination resulted in the highest expression of *chlorophyll b reductase* (BRADI1G13416), which catalyzes the first step in the conversion of chlorophyll b to a, and *pheophorbide a oxygenase* (BRADI3G53860 and BRADI1G75270), which produces red chlorophyll catabolite from pheophorbide a (Barry, 2009) (Table S2). Maintenance of higher or comparable levels of chlorophyll content under salinity treatments (i.e. all stress combinations except for D&H) at 4 and 12 DAA, may be attributed to an average decrease of 48% in leaf area, compared with non-salinity treatments (Shaar-Moshe *et al.*, 2017). Nevertheless, leaf size and chlorophyll content showed no association ($r$ = -0.6, $P$ = 0.32).

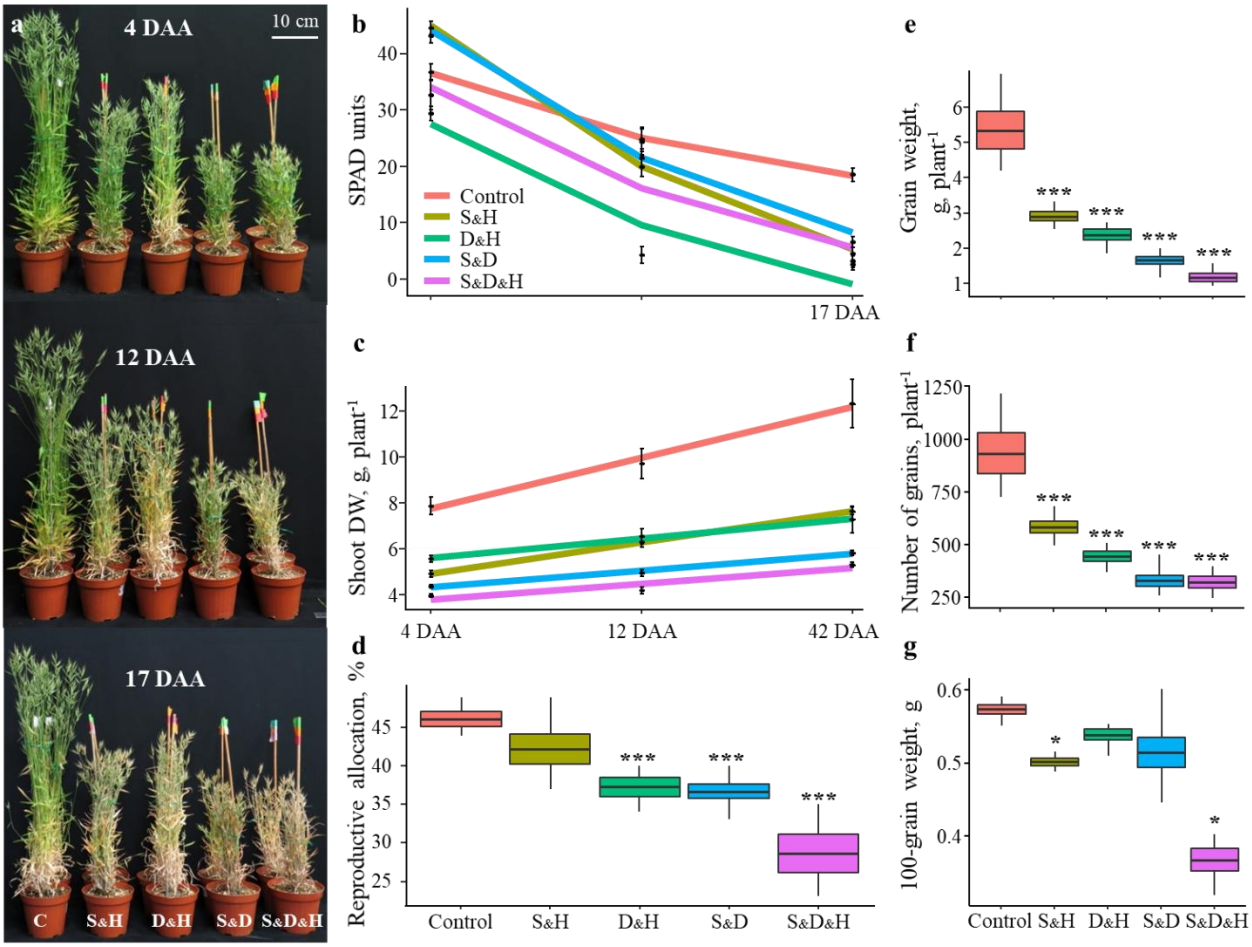


**Figure 1** Performance traits and fitness of *Brachypodium distachyon* plants grown under control (C) and combinations of stresses: salinity and heat (S&H), drought and heat (D&H), salinity and drought (S&D), salinity, drought and heat (S&D&H). (**a**) Plants grown under control conditions and four combinations of stresses at three developmental stages during the reproductive stage: 4, 12 and 17 days after anthesis (DAA). (**b**) Chlorophyll content at 4, 12, and 17 DAA, under control and combinations of stresses. (**c**) Accumulation pattern of shoot dry weight (DW) at 4, 12, and 42 DAA. (**d**) Box plots of reproductive allocation, (**e**) grain weight, (**f**) number of grains per plant, and (**g**) 100-grain weight. * and *** indicate significant differences between control and stress treatments at $P \leq 0.05$ and 0.001, respectively, as determined by Dunnet's test. Values are mean ($n$=4)±SE.

To assess the effects of the stress combinations on plant fitness and its performance traits, we measured shoot dry weight (DW) along three reproductive stages, 4 ,12 and 42 DAA (i.e. plant senescence), and reproductive output at 42 DAA. In general, under all combined stresses plants accumulated significantly less shoot DW. A closer examination of the acclimation response showed that under D&H and salinity and heat (S&H) plants accumulated on average 34% more DW than under (salinity and drought) S&D and (salinity, drought and heat) S&D&H, at all three developmental stages. During the reproductive stages the vegetative growth of cereals is ceased,

thus, accumulation of shoot DW is ascribed to an increase in the reproductive tissues and subsequently in grain weight. Analysis of relative growth, between 4 and 42 DAA, found a similar average increase in DW of ~55% under control and $S_{\&}H$, while all other combined stresses showed a milder increase in DW of only ~33% during the reproductive stages (Fig. 1c). Consistently, the proportion of reproductive output per shoot DW, which was used as a surrogate for reproductive allocation, was similar between $S_{\&}H$ and control conditions. The other stress combinations, and especially $S_{\&}D_{\&}H$, displayed significant reductions compared with control (Fig. 1d). To further investigate the differences of the reproductive output among the combined stresses, we examined yield parameters: total grain weight and number, and 100-grain weight. Total grain weight and number showed a similar pattern of gradual decreases as shoot DW, with $S_{\&}H$ showing limited impairment and $S_{\&}D_{\&}H$ exhibiting sever impairment (Fig. 1e, f). However, this pattern was not observed upon examination of 100-grain weight, which was maintained at levels comparable to control under $D_{\&}H$ and $S_{\&}D$ (Fig. 1g). As shoot DW accumulated to similar values under $S_{\&}H$ and $D_{\&}H$, the difference in the reproductive allocation between the two combinations, can be attributed to higher values of total grain weight and number under $S_{\&}H$ (Fig. 1c-f). Examination of grain viability, of grains that developed on plants subjected to combinations of stresses, revealed a severe impairment in germination rate only under $S_{\&}D$ and $S_{\&}D_{\&}H$, compared with control (Fig. S1).

**$D_{\&}H$ resulted in a rapid reduction of chlorophyll florescence**

To investigate the effects of the combined stresses on the photosynthetic apparatus and its associated pigments, we measured maximal photochemical efficiency of photosystem II (PSII) (*Fv*/*Fm*), at three developmental stages. Under $S_{\&}D_{\&}H$ and $D_{\&}H$, plants exhibited a similar pattern of comparable declines of ~12 and 92% in *Fv*/*Fm*, compared with control, at 12 and 17 DAA, respectively (Fig. 2a; Table S1). Physiological responses and acclimations are the consequences of orchestrated transcriptional changes. Therefore, we examined the association between the physiological trait and its underlying transcriptional pattern of specific functional gene-subsets. This analysis revealed that the physiological changes in PSII efficiency were correlated with expression patterns of genes involved in light harvesting complex (LHC) and polypeptide subunits of PSII (Fig. 2a, b; Table S2).

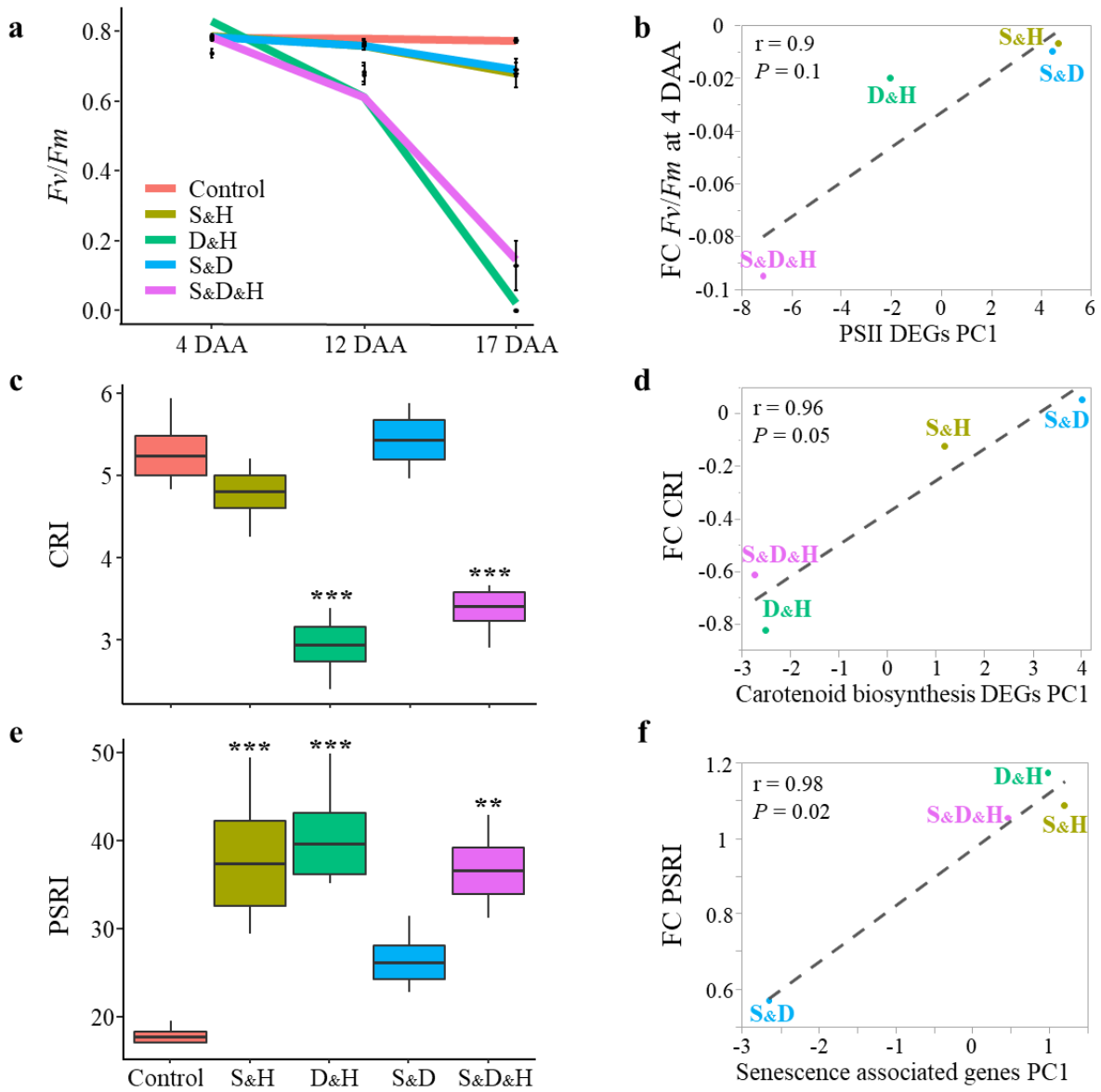


**Figure 2** Differential effects of combined stresses on photosynthetic apparatus, its associated pigments and the progression of senescence at the physiological and transcriptional levels. (**a**) maximal photochemical efficiency of photosystem II (*Fv*/*Fm*), at 4, 12, and 17 DAA, under control and combinations of stresses. (**b**) Correlation between first principle component (PC1) of expression pattern of genes related to photosystem II (PSII) and fold change (FC) values of *Fv*/*Fm* at 4 DAA. (**c**) Box plots of carotenoid reflectance index (CRI) are calculated as 1/W510 - 1/W550. W represents the wavelengths used to calculate the reflectance index. (**d**) Correlation between PC1 of expression pattern of genes involved in carotenoid synthesis and FC values of carotenoid content. (**e**) Plant senescence reflectance index (PSRI) is calculated as [(W680-W500) / W750] × 1000. (**f**) Correlation between PC1 of expression pattern of senescence associated genes (SAGs) and PSRI. ** and *** indicate significant differences between control and stress treatments at $P<0.01$ and 0.001, respectively, as determined by Dunnet's test. Values are mean ($n$=4)±SE. Growth conditions are as follows: salinity and heat (S&H), drought and heat (D&H), salinity and drought (S&D), salinity, drought and heat (S&D&H).

**S&H and S&D differentially affect leaf senescence and carotenoid content**

Carotenoids have a structural role in the assembly of the photosynthetic apparatus, and the retention of carotenoids, in the progress of chlorophyll breakdown during senescence, has been suggested as a mechanism of photoprotection (Nisar *et al.*, 2015). To assess carotenoid content, we used the non-destructive carotenoid reflectance index 1 (CRI1) (Gitelson *et al.*, 2002). Under D&H and S&D&H, plants exhibited low values of CRI1, whereas under S&H and S&D, CRI1 values were comparable to control (Fig. 2c). Carotenoid content exhibited a high and positive association with expression pattern of genes involved in carotenoid metabolism under the combined stresses (Fig. 2d; Table S2).

Plant senescence reflectance index (PSRI), which estimates the proportion between chlorophyll and carotenoids (Merzlyak *et al.*, 1999), was used to quantitatively evaluate leaf senescence. All stress combinations, except for S&D, showed higher values of PSRI, compared with control, indicating stress induced-senescence (Fig. 2e). This pattern was also reflected at the transcriptional level by a strong association between PSRI and senescence associated genes (SAG). In addition, a high correlation (r = 0.97, $P$ = 0.03) was detected between PSRI and genes involved in chloroplast nucleoid metabolism and maintenance (Table S2), a pathway that was enriched among genes uniquely expressed only under stress combinations (Shaar-Moshe *et al.*, 2017). The different PSRI values that were detected between S&H and S&D might be attributed to a higher carotenoid content under S&D, as chlorophyll contents were comparable under these stress combinations (Figs 1b, 2c). Consistently, mRNA levels of *phytoene synthase* (*PSY*, BRADI4G37520), a rate-limiting enzyme, which catalyzes the first committed step in carotenogenesis (Hirschberg, 2001), were up-regulated only under S&D (Table S2).

**ROS levels diminished under combinations of stresses**

Reactive oxygen species (ROS), which are regulators of various processes, including stress signaling and development, were shown to increase under abiotic stresses (Miller *et al.*, 2010). Our result showed that under all stress combinations plant accumulated between 46 to 84%, less ROS, compared with control (Fig. 3a). ROS are also toxic byproducts of aerobic metabolism (e.g. photosynthesis, photorespiration, and respiration) that are detoxified by an array of enzymatic and non-enzymatic antioxidants (Mittler, 2017). ROS levels, showed positive correlations with photosynthesis rate (r = 0.92, $P$ = 0.03, Fig. S2a), as well as with shoot DW (Fig. 3b) and grain

weight (r = 0.94, $P$ = 0.02, Fig. S2b). ROS levels showed no correlation with expression patterns of genes involved in oxidative stress and redox metabolism, either all annotated DEGs (Fig. 3c) or functional subcategories (e.g. respiratory burst, glutaredoxins, dismutases and catalases, Table S2). Furthermore, metabolites that function as ROS scavenging, such as: ascorbic acid and glutathione, were not detected in the metabolic analysis (Table S3). To validate the transcriptional correlations, we assessed the transcriptional signatures, related to ROS origin and type by ROSMETER tool (Rosenwasser *et al.*, 2013). This analysis also provided limited correlation with specific ROS (Fig. S2c).

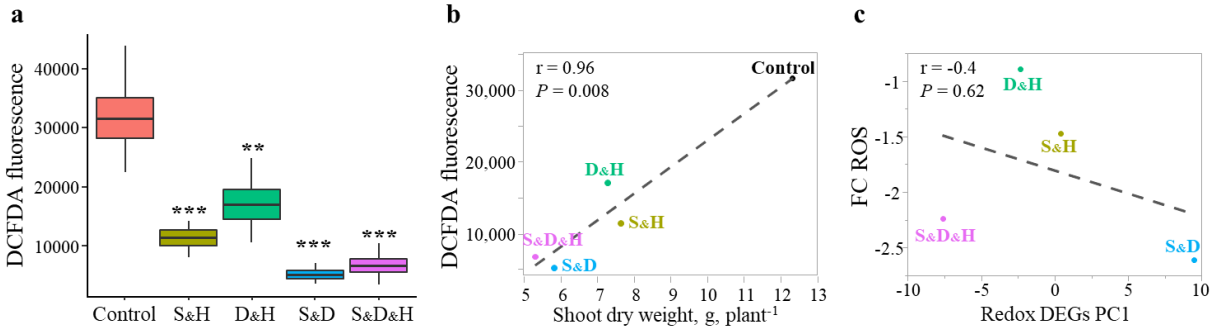


**Figure 3** Reactive oxygen species (ROS) content and its association with physiological traits or gene expression pattern. (**a**) Box plot of ROS content that was assessed by $H_2$DCFDA fluorescence. ** and *** indicate significant differences between control and stress treatments at $P$<0.01 and 0.001, respectively, as determined by Dunnet's test. Values are mean ($n$=5)±SE. (**b**) Correlation between shoot dry weight and ROS content. (**c**) Correlation between first principle component (PC1) of expression pattern of genes involved in oxidative stress and redox metabolism, and fold change (FC) values of ROS content. Growth conditions are as follows: salinity and heat (S&H), drought and heat (D&H), salinity and drought (S&D), salinity, drought and heat (S&D&H).

## Starch content depleted under heat-related stress combinations

Under abiotic stresses, such as salinity, drought and heat, starch is usually degraded to support the plant energy demands and carbon supply at times when photosynthesis is limited (Thalmann & Santelia, 2017). This process resulted in the accumulation of maltose, a major degrading product of starch, and of its deriving sugars (Thalmann *et al.*, 2016). Under all heat-related stress combinations, plants accumulated less starch in their leaves, compared with control conditions (ranging between 65% to 97%; Fig. 4, Fig. S3a). This pattern of starch attenuation, correlated with expression pattern of starch synthesis and degradation DEGs (Table S2, Fig. S3b), suggesting a tight regulation, of both anabolic and catabolic processes. In addition, starch was in a close

association with maltose content (r = 1, $P$ = 0.004, Fig. S3c). Starch content in the leaves did not correlate with photosynthesis rate (r = 0.62, $P$ = 0.3, Fig. S3d) or with grain weight (r = 0.54, $P$ = 0.3, Fig. S3e). The plasticity of starch attenuation may imply the occurrence of specific shifts in the balance between defense, maintenance and reproductive processes under each stress combination.

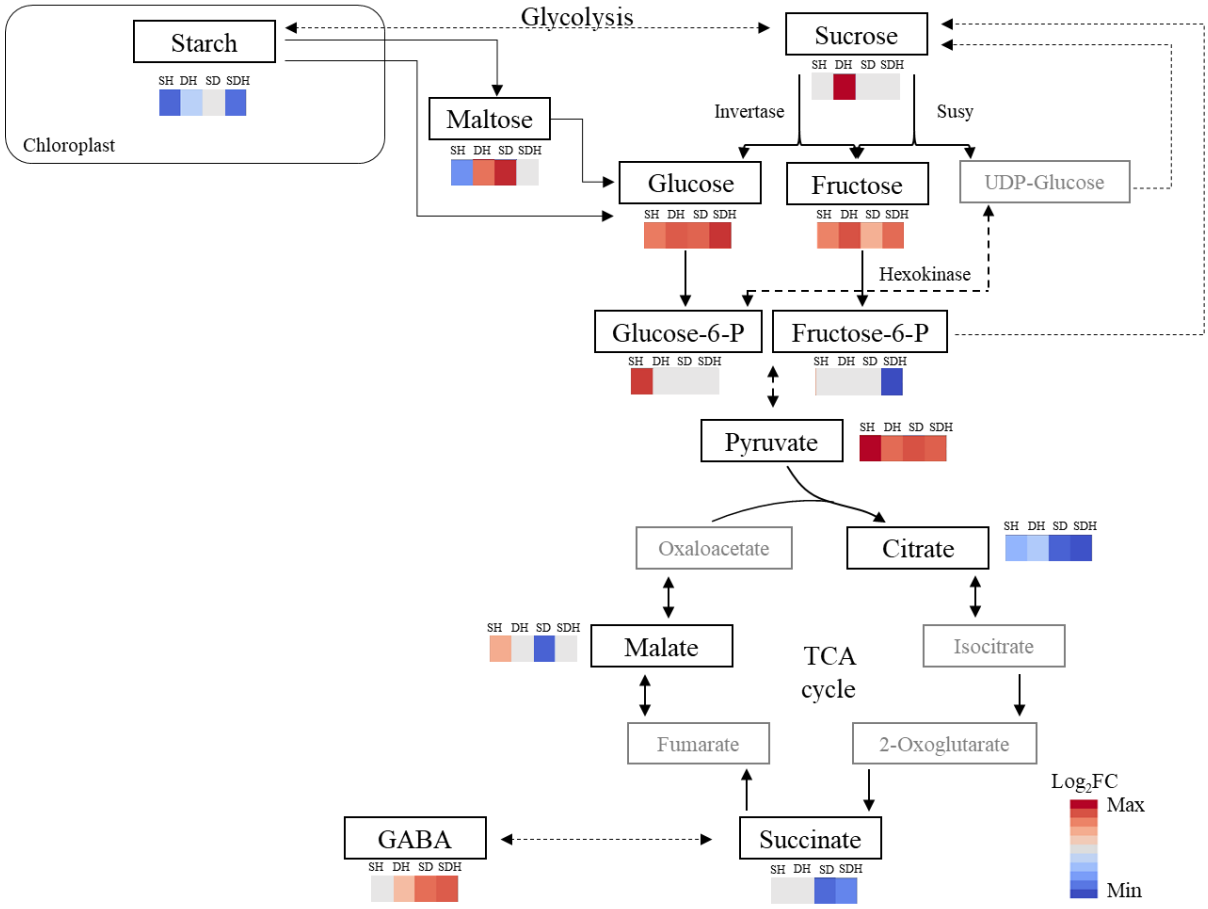


**Figure 4** Accumulation patterns of metabolites involved in energy metabolism in *Brachypodium distachyon* plants grown under control and combinations of stresses: salinity and heat ($S_{\&}H$), drought and heat ($D_{\&}H$), salinity and drought ($S_{\&}D$), salinity, drought and heat ($S_{\&}D_{\&}H$). Red and blue colors indicate accumulation and depletion in metabolite content, respectively, and white color indicates a non-significant change, compared with control.

**Plant energy balance is severely impaired under S&D and S&D&H**

To improve our understanding on cellular energy metabolism under stress, we performed a complete foliar metabolic profiling, in parallel with the transcriptional analysis. Among the 69 annotated metabolites, differentially accumulated under at least one stress combination, most metabolites (94%) showed the same response pattern (i.e. accumulation or depletion), across the four combinations. However, plants exhibited differences in the intensity of metabolite accumulation or depletion (e.g. GABA, tryptophan and mannose reached FC differences of 71, 48, and 22, respectively, compared with control conditions, Table S3). Functional classification of the metabolic data revealed that sugars, sugar phosphates and sugar alcohols constituted up to 41% of the metabolites and enrichment analysis further identified galactose metabolism as a prevalent pathway under stress. This pathway includes sugars with various functions such as: signaling (e.g. glucose and fructose), transport (sucrose and raffinose), osmoprotectants (e.g. galactinol and myo-inositol), cell wall polysaccharides (e.g. galactose and mannose) and glycerolipid metabolism (e.g. galactosylglycerol), which showed distinct metabolic responses under each stress combination (Fig. S4).

We further focused our analysis on metabolites involved in cellular respiration. Sucrose and its two hexoses constitute the early steps of glycolysis, the first stage of respiration. Plants accumulated sucrose only under D&H (FC = 1.2). While its breakdown products, the hexoses fructose and glucose, accumulated under all combined stresses (Fig. 4, Table S3). The hexoses are further converted to glucose-6-P that accumulated under S&H (FC = 2.2) and fructose-6-P, which depleted under S&D&H (FC = -4.6). The end products of glycolysis include the organic acid pyruvate that accumulated to comparable levels under all stress combinations and malate, which accumulated under S&H and decreased under S&D (FC= 1.8 and -3.4, respectively). Additional organic acids of the tricarboxylic acid (TCA) cycle, showed reduced levels under the combined stresses. For example, succinate, a metabolite connecting TCA cycle and (γ-Aminobutyric acid) GABA shunt (Fait *et al.*, 2007), showed decreased levels only under S&D and S&D&H. Consistently, high levels of GABA were detected in leaves of plants subjected to these two stresses (Fig. 4, Table S4).

**Preferable accumulation of osmolytes under combined stresses**

Accumulation of compatible solutes is an adaptive mechanism that mitigates the deleterious effects of an osmotic stress by sustaining cellular turgor and water status and protecting cellular constituents (Rontein *et al.*, 2002). Under all combined stresses, an increase in osmotic adjustment (OA) was detected, predominantly under S&D and S&D&H. However, this increment was not sufficient to retain leaf relative water content (RWC), to a level comparable to control conditions. Heat stress did not contribute to the OA, as indicated by the similar values of OA under S&D and S&D&H, but it led to a dramatic loss of 20% in leaf RWC under S&D&H compared with S&D (Fig. 5a).

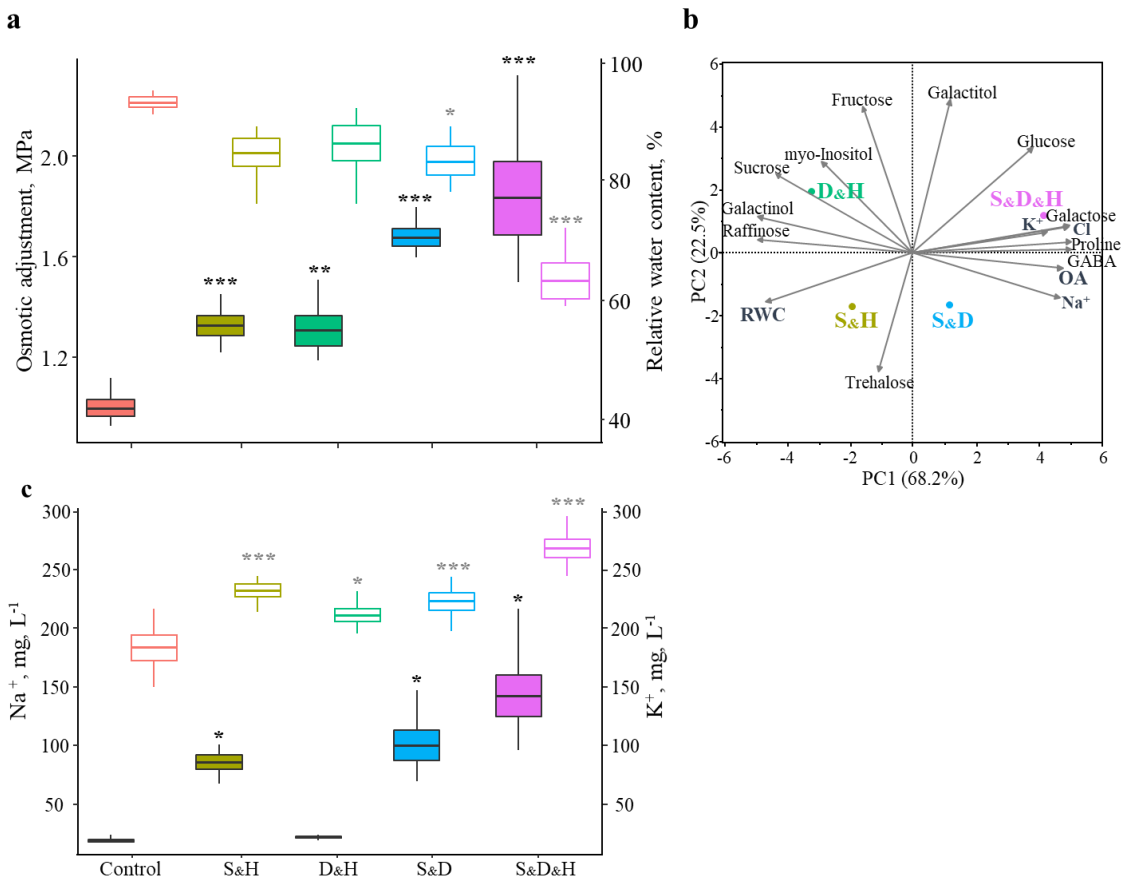


**Figure 5** The contribution of osmolytes to osmotic adjustment (OA) and its relationship with relative water content (RWC). (**a**) Box plot of OA and leaf RWC, denoted by filled and empty boxes, respectively. (**b**) Biplot of a principal component (PC) analysis of the relationship among osmolytes (i.e. 11 organic osmolytes, detected by metabolic profiling, and three ions) and the physiological traits OA and RWC, on the four combined stresses. (**c**) Box plot of $Na^+$ and $K^+$ concentrations, denoted by filled and empty boxes, respectively. *, ** and *** indicate significant differences between control and stress treatments at $P \leq 0.05$, 0.01 and 0.001, respectively, as determined by Dunnet's test. Values are mean ($n$=6)±SE. Growth conditions are as follows: salinity and heat (S&H), drought and heat (D&H), salinity and drought (S&D), salinity, drought and heat (S&D&H).

To gain a comprehensive understanding on the osmolytes (i.e. metabolites and ions) that contributed to OA and its relationship with RWC, we performed a principle component analysis (PCA). The cumulative contribution of the two major principal components (PCs, Eigenvalues > 1), to the total variation, was 91%. PC1 that explained 68.2% of the variation was loaded positively with OA, the metabolites proline, GABA, galactose and glucose, and the ions $Na^+$, $K^+$ and $Cl^-$, suggesting the involvement of these osmolytes in osmoregulation. On the other hand, PC1 was loaded negatively with RWC, raffinose, galactinol, sucrose and myo-Inositol, indicating the negative association between OA and RWC and implying that these metabolites did not contribute to osmotic adjustment in *B. distachyon* (Fig. 5b). The lack of correlation between OA and fructose, galactitol and trehalose may result from additional functions these metabolites hold, such as signaling and transport (Ruan, 2014). Cumulative fold-changes (FC) of significant compatible solutes revealed their gradual accumulation across the combined stresses, ranging between 39, under $S_{\&}H$, and reaching up to 129 cumulative FC, under $S_{\&}D_{\&}H$ (Table S3). Although $S_{\&}H$ and $D_{\&}H$ had comparable levels of OA (Fig. 5a), under $D_{\&}H$ plants accumulated a higher level of compatible solutes compared with $S_{\&}H$ (i.e. cumulative FC of 50 *versus* 39, respectively).

Salt-treated plants accumulated higher levels of $Na^+$ in their leaves compared with control and $D_{\&}H$. Accumulation of $K^+$, which was positively correlated with both $Na^+$ and $Cl^-$ accumulation, was detected under all combined stresses, especially in plants subjected to $S_{\&}D_{\&}H$ that accumulated 45% more $K^+$, compared with control (Fig. 5c). The accumulation patterns of $K^+$ and $Na^+$ across the combined stresses, resulted in a similar four-fold reduction in $K^+$/ $Na^+$ ratio among the salt-treated plants (Fig. S5a). In addition, $Cl^-$ was accumulated under all combined stresses, primarily in plants subjected to $S_{\&}D_{\&}H$, which accumulated twice the amount of $Cl^-$, compared with control conditions (Fig. S5b).

# Discussion

Plant acclimations to abiotic stress conditions occur through a coordinated sequence of transcriptional, translational, metabolic and physiological events, from the cellular to the whole plant level. These processes change the metabolic status of the plants toward a new steady-state level that supports plant growth and fitness under the unfavorable conditions (Chaves *et al.*, 2009). To study acclimation mechanisms of temperate grasses to combinations of abiotic stresses, we subjected *B. distachyon* plants to combinations of three prevalent environmental constrains at the Mediterranean region (i.e. combinations of salinity, drought and heat) (Vautard *et al.*, 2007; Maggio *et al.*, 2011). We examined the extent of phenotypic and metabolic plasticity and the limitation such conditions imposed on plant performances and fitness. This analysis revealed commonalities and divergences between the stress combinations and specific acclimation and life-history strategy plants elicited under each combination.

**Plants under $D_{\&}H$ exhibited life-history strategy of accelerated senescence**

The Mediterranean-like environments are usually affected by prolonged water stress combined with heat waves, causing together extensive agricultural losses (Loss & Siddique, 1994). Under such conditions, annual plants that have a rapid life cycle and escape the spring heat waves may gain a high fitness. The *B. distachyon* accession 21-3 that was collected in northern Iraq is native to an area with low winter precipitation and high summer temperatures (exceeding 35°C) (Fig. S6; Des Marais & Juenger, 2016). Accordingly, under $D_{\&}H$, plants exhibited an accelerated senescence that was manifested by a significant reduction in chlorophyll content, starting as early as 4 DAA (Fig. 1b), a reduction in photosynthesis rate (Shaar-Moshe *et al.*, 2017), accumulation of galactosylglycerol, consistent with breakdown of thylakoid membranes, which contain up to 80% galactosylglycerolipids (Holzl & Dormann, 2007), and accumulation of transport sugars (e.g. sucrose and galactitol) (Fig. 4, Table S3, Fig. S4). Leaf senescence, which is characterized by the transition from nutrient assimilation to nutrient remobilization, involves, in its early phase, breakdown of chloroplasts and decrease in photosynthesis (Avila-Ospina *et al.*, 2014). The positive correlation between leaf senescence (measured by PSRI) and expression pattern of genes involved in chloroplast nucleoid metabolism and maintenance provides a transcriptional support for the link between leaf aging and chloroplast stability. Despite a reduction in photosynthesis, the hexoses, glucose and fructose accumulated under $D_{\&}H$ (Fig. 4, Table S3). This may occur through starch

degradation or through a decrease in amino acid synthesis, which leads to a higher carbon availability (Jongebloed *et al.*, 2004). Indeed, under $D_{\&}H$, starch level depleted, compared with control conditions, and the amino acids tryptophan and GABA, only mildly accumulated, compared with plants grown under the other combined stresses (Table S3). In addition, considering that up to 70% of the leaf proteins are localized within the chloroplasts, the recycling and management of materials accumulated during leaf development into exportable nutrients, is a critical process in senescing plants to sustain yield and fitness (Sade *et al.*, 2018). The accumulation of transport sugars that can move through the phloem to the filling grains may indicate that nutrient remobilization was accelerated under $D_{\&}H$. Nevertheless, nutrient reservoir and/ or their transport rate did not meet the progression of senescence, resulting in a reduction of 19% in the reproductive allocation and a decreased in total grain weight (Fig. 1d-e). This life-history strategy of accelerated senescence resulted in a trade-off in the reproductive allocation via shortened grain-filling period, which consequently diminished grain yield.

**Plants grown under $S_{\&}H$ exhibited moderate effects of the stress on functional and performance traits**

Plants subjected to $S_{\&}H$ were able to sustain, for a longer period, higher or comparable values of chlorophyll content and *Fv*/*Fm* ratio, respectively, compared with control plants (Figs 1b, 2a), which further support the moderate decreases in photosynthesis rate (Shaar-Moshe *et al.*, 2017). Under $S_{\&}H$ plants accumulated 29% less shoot DW, similarly to $D_{\&}H$, yet the reproductive allocation was comparable to control conditions, indicating that the plants maintained source-sink relationships and successfully partitioned photosynthetic assimilates to the reproductive tissues (Fig. 1c, d).

Plants grown under $S_{\&}H$ also maintained leaf water content at a level comparable to control conditions, possibly through an increase in OA (Fig. 5a). By increasing intercellular osmolarity plants maintain high cellular turgor necessary for cell expansion and facilitate a higher stomatal conductance under lower water potentials, thus actively modifying the environment they experience. OA can be achieved through *de-novo* synthesis of compatible solutes and through accumulation of inorganic ions. Compatible solutes, which defined as small water-soluble molecules devoid of metabolic effects, can also function in osmoprotection of cellular structures, by interacting with membranes, protein complexes, or enzymes (Bohnert *et al.*, 1995). OA, which

occurred under all stress combinations, has increased with the aggravation of the stresses (Fig. 5A) and is proportional to the reduction in plant water status (Blum, 2017). In accordance, accumulation of compatible solutes such as glucose, proline and GABA, was positively correlated with OA, and exhibited a higher accumulation under $S_{\&}D$ and $S_{\&}D_{\&}H$, and a lower accumulation under $S_{\&}H$ and $D_{\&}H$ (Fig. 5b, Table S3). Plants' ability to retain a high water content under $S_{\&}H$, despite a relative mild increase in compatible solutes accumulation, may be attributed to an increase in inorganic osmolytes such as $K^+$ and especially $Na^+$ that are non-competitive to growth (Figs 5c, S5). As *de novo* synthesis of osmolytes is an energetically expensive process that only contributes to the fine adjustment of cellular osmotic potential, accumulation of ions for OA can mitigate the energy trade-off between defense mechanisms and reproductive output and prioritize the latter, thus minimizing yield penalty under $S_{\&}H$ (Shabala & Shabala, 2011).

**Plant energy balance was severely damaged under combinations of $S_{\&}D$ and $S_{\&}D_{\&}H$**

Soil salinity is a growing concern in arid and semi-arid regions, both in cultivated land and natural habitats, leading to severe reductions in plant growth and productivity (Rozema & Flowers, 2008). Limited water availability can impair Hill reaction, evaporative coolant and mass flow of solvents, from both the soil and source tissues (Bohnert *et al.*, 1995). Indeed, under $S_{\&}D$ and $S_{\&}D_{\&}H$, plants were not able to retain a high RWC as control plants (Fig. 5b), and photosynthesis and transpiration rates dropped by $\geq$ 82 and 90%, respectively. In accordance, leaf temperature increased significantly compared with either control or single heat stress (Shaar-Moshe *et al.*, 2017), implying limited ability of the plants to cool their leaves by transpiration. $S_{\&}D$ and $S_{\&}D_{\&}H$ also led to sever growth attenuations and to a decrease in the reproductive output by 63 and 74%, respectively (Fig. 1c-g). Similar effects of reduction in plant growth and productivity, were reported for wild (*Hordeum spontaneum*) and domesticated barley (*Hordeum vulgare*) subjected to $S_{\&}D$ during the vegetative and reproductive stages (Ahmed *et al.*, 2012; Ahmed *et al.*, 2013).

ROS accumulation that was reduced under all combinations of stresses was tightly correlated with photosynthesis rate, shoot DW and grain weight and not with expression patterns of genes involved in oxidative stress and redox metabolism or with antioxidative metabolites (Fig. 3, Tables S2, S3, Fig. S3). Several studies have demonstrated that reduction of ROS levels below a certain threshold could result in suppression of cellular proliferation and negatively affect differentiation and immunity (Mittler, 2017). Given that ROS production is a universal consequence of cellular

metabolism (e.g. photosynthesis, photorespiration, and respiration), a decrease in these processes could subsequently lead to a decrease in ROS levels. We therefore speculate that under the experimental procedure, ROS level can serve as an indicator of the metabolic status of the plants, further highlighting the damages that occurred in the plants under combined stresses and especially under $S_{\&}D$ and $S_{\&}D_{\&}H$.

Sink strength is of a paramount importance for grain filling. The developing grains are mainly depended on two sources of assimilates: photosynthesis after anthesis and translocation of reservoirs assimilated before anthesis and temporarily stored in the stem. Under stress conditions, which diminish photosynthesis capacity of source tissues, grain filling is largely dependent on remobilization of stem reserves (Gallagher *et al.*, 1976). The prolonged stress conditions, imposed under $S_{\&}D$ and $S_{\&}D_{\&}H$, severely curtailed photosynthesis capacity and shifted the balance from maintenance and reproduction towards defense processes throughout the plants' life history. As a consequence of the decreased photosynthesis and culm length (Shaar-Moshe *et al.*, 2017), these plants are expected to contain less stem reserves (Borrell *et al.*, 1993) that are essential for grain filling and source-sink homeostasis (Jagadish *et al.*, 2015).

The effect of phenotypic plasticity on plant fitness, can be positive, neutral or maladaptive (van Kleunen & Fischer, 2005). Thus, not all alterations lead to the desired outcome of ameliorating the unfavorable conditions (Donohue, 2003). The limited water availability, under $S_{\&}D$ and $S_{\&}D_{\&}H$, could result in attenuation of shoot DW accumulation (Fig 1A), which leads to accumulation of sugars, such as glucose and galactose (Fig. 4, Table S3), due to a decreased demand (Hummel *et al.*, 2010). Sugar accumulation can also result in feedback inhibition of photosynthesis (Rossi *et al.*, 2015). Depletions of metabolites of the TCA cycle, such as citrate and succinate under $S_{\&}D_{\&}H$, and malate under $S_{\&}D$, further suggest that cellular respiration and thus plant energy balance, were compromised under these combinations. GABA, which has been shown to accumulate under abiotic and biotic stresses and is associated with diverse physiological responses, including fluxes of carbon into the TCA cycle, nitrogen metabolism and osmoregulation (Bouche & Fromm, 2004), was largely produced under $S_{\&}D$ and $S_{\&}D_{\&}H$ (Fig. 4, Table S3). Since GABA shunt is closely connected to the TCA cycle (Fait *et al.*, 2007), the surplus accumulation of GABA, under $S_{\&}D$ and $S_{\&}D_{\&}H$, may result from a decline in respiration. Altogether, the morph-physiological traits and metabolic profiling demonstrate the aggravating effects of the combined

stresses, which hamper plant performances, diminish their fitness and may impend their dispersion in areas prone to simultaneous occurrence of salinity and drought with or without heat stress.

**Concluding remarks**

The prevalence of different combinations of stresses in the field, and their projected increase in frequency and intensity (Suzuki *et al.*, 2014; Zandalinas *et al.*, 2018), challenges the common methodology of single stress treatments and the relevance of such assays to plant acclimation under natural and agricultural systems (Reguera *et al.*, 2012). The variable and unpredictable environmental conditions that are associated with climate change, force plants to rapidly acclimate, both within and across generations (Nicotra *et al.*, 2010). Understanding the effects of environmental constraints on plant life-history strategies and the limits of plasticity under changing environments can assist in predicting species dispersion and management, and facilitate the development of varieties, which are better adapted to the foreseen climatic conditions. To meet these challenges, a multidisciplinary approach that considers physiological and phenological information of realistic stress assays, together with system regulatory mechanisms, from the genes to the whole plant level, should be undertaken.

## Acknowledgments

We thank A. Oksenberg, I. Vilan, I. Ayalon and I. Sabag for technical assistance with the physiological experiments and N. Jayasinghe for analysis of metabolic samples. GC-MS analysis was carried out at Metabolomics Australia, School of BioSciences, University of Melbourne, which is supported by funds from the Australian Government's National Collaborative Research Infrastructure Scheme (NCRIS) administered through Bioplatforms Australia (BPA) Ltd. This research partially supported by the United States-Israel Binational Science Foundation (BSF) (grant #2011310) and the Hebrew University of Jerusalem. LSM is indebted to the Israeli President's Scholarship for Scientific Excellence and Innovation.

# References


**Ahmed IM, Cao F, Zhang M, Chen X, Zhang G, Wu F. 2013.** Difference in yield and physiological features in response to drought and salinity combined stress during anthesis in Tibetan wild and cultivated barleys. *PLoS One* **8**: e77869.

**Ahmed IM, Dai H, Zheng W, Cao F, Zhang G, Sun D, Wu F. 2012.** Genotypic differences in physiological characteristics in the tolerance to drought and salinity combined stress between Tibetan wild and cultivated barley. *Plant Physiology and Biochemistry* **63**: 49-60.

**Avila-Ospina L, Moison M, Yoshimoto K, Masclaux-Daubresse C. 2014.** Autophagy, plant senescence, and nutrient recycling. *Journal of Experimental Botany* **65**: 3799-3811.

**Barhoumi Z, Atia A, Rabhi M, Djebali W, Abdelly C, Smaoui A. 2010.** Nitrogen and NaCl salinity effects on the growth and nutrient acquisition of the grasses *Aeluropus littoralis*, *Catapodium rigidum*, and *Brachypodium distachyum*. *Journal of Plant Nutrition and Soil Science* **173**: 149-157.

**Barry CS. 2009.** The stay-green revolution: recent progress in deciphering the mechanisms of chlorophyll degradation in higher plants. *Plant Science* **176**: 325-333.

**Bazzaz FA, Chiariello NR, Coley PD, Pitelka LF. 1987.** Allocating resources to reproduction and defense. *Bioscience* **37**: 58-67.

**Benjamini Y, Hochberg Y. 1995.** Controlling the false discovery rate: a practical and powerful approach to multiple testing. *Journal of the Royal Statistical Society. Series B (Methodological)* **57**: 289-300.

**Bian YW, Deng X, Yan X, Zhou JX, Yuan LL, Yan YM. 2017.** Integrated proteomic analysis of *Brachypodium distachyon* roots and leaves reveals a synergistic network in the response to drought stress and recovery. *Scientific Reports* **7**: 46183.

**Blum A. 2017.** Osmotic adjustment is a prime drought stress adaptive engine in support of plant production. *Plant Cell and Environment* **40**: 4-10.

**Bohnert HJ, Nelson DE, Jensen RG. 1995.** Adaptations to environmental stresses. *Plant Cell* **7**: 1099-1111.

**Borrell AK, Incoll LD, Dalling MJ. 1993.** The influence of the *Rht1* and *Rht2* alleles on the deposition and use of stem reserves in wheat. *Annals of Botany* **71**: 317-326.

**Bouche N, Fromm H. 2004.** GABA in plants: just a metabolite? *Trends in Plant Sciences* **9**: 110-115.

**Bradshaw AD. 1965.** Evolutionary significance of phenotypic plasticity in plants. *Advances in Genetics* **13**: 115-155.

**Cao J, Jiang M, Li P, Chu Z. 2016.** Genome-wide identification and evolutionary analyses of the *PP2C* gene family with their expression profiling in response to multiple stresses in *Brachypodium distachyon*. *BMC Genomics* **17**: 175.

**Chaves MM, Flexas J, Pinheiro C. 2009.** Photosynthesis under drought and salt stress: regulation mechanisms from whole plant to cell. *Annals of Botany* **103**: 551-560.

**De Deyn GB. 2017.** Plant life history and above-belowground interactions: missing links. *Oikos* **126**: 497-507.

**Des Marais DL, Juenger TE 2016.** *Brachypodium* and the abiotic environment. In: Vogel J ed. *Genetics and Genomics of Brachypodium*. Cham, Switzerland: Springer, 291-311.

**Des Marais DL, Lasky JR, Verslues PE, Chang TZ, Juenger TE. 2017.** Interactive effects of water limitation and elevated temperature on the physiology, development and fitness of diverse accessions of *Brachypodium distachyon*. *New Phytologist* **214**: 132-144.

**Dias DA, Hill CB, Jayasinghe NS, Atieno J, Sutton T, Roessner U. 2015.** Quantitative profiling of polar primary metabolites of two chickpea cultivars with contrasting responses to salinity. *Journal of Chromatography B* **1000**: 1-13.

**Donohue K. 2003.** Setting the stage: phenotypic plasticity as habitat selection. *International Journal of Plant Sciences* **164**: S79-S92.

**Fait A, Fromm H, Walter D, Galili G, Fernie AR. 2007.** Highway or byway: the metabolic role of the GABA shunt in plants. *Trends in Plant Sciences* **13**: 14-19.

**Gallagher JN, Biscoe PV, Hunter B. 1976.** Effects of drought on grain-growth. *Nature* **264**: 541-542.

**Gitelson AA, Zur Y, Chivkunova OB, Merzlyak MN. 2002.** Assessing carotenoid content in plant leaves with reflectance spectroscopy. *Photochemistry and Photobiology* **75**: 272-281.

**Grime JP. 1977.** Evidence for the existence of three primary strategies in plants and its relevance to ecological and evolutionary theory. *The American Naturalist* **111**: 1169-1194.

**Hill CB, Dias DA, Roessner U. 2015.** Current and emerging applications of metabolomics in the field of agricultural biotechnology. *Advances in Food Biotechnology*: 13-26.

**Hirschberg J. 2001.** Carotenoid biosynthesis in flowering plants. *Current Opinion in Plant Biology* **4**: 210-218.

**Holzl G, Dormann P. 2007.** Structure and function of glycoglycerolipids in plants and bacteria. *Progress in Lipid Research* **46**: 225-243.

**Hong SY, Park JH, Cho SH, Yang MS, Park CM. 2011.** Phenological growth stages of *Brachypodium distachyon*: codification and description. *Weed Research* **51**: 612-620.

**Hummel I, Pantin F, Sulpice R, Piques M, Rolland G, Dauzat M, Christophe A, Pervent M, Bouteille M, Stitt M, et al. 2010.** Arabidopsis plants acclimate to water deficit at low cost through changes of carbon usage: an integrated perspective using growth, metabolite, enzyme, and gene expression analysis. *Plant Physiology.* **154**: 357-372.

**Jagadish KSV, Kishor PBK, Bahuguna RN, von Wiren N, Sreenivasulu N. 2015.** Staying alive or going to die during terminal senescence-an enigma surrounding yield stability. *Frontiers in Plant Science* **6**: 1070.

**Jang SJ, Wi SJ, Choi YJ, An G, Park KY. 2012.** Increased polyamine biosynthesis enhances stress tolerance by preventing the accumulation of reactive oxygen species: T-DNA mutational analysis of *Oryza sativa* lysine decarboxylase-like protein 1. *Molecules and Cells* **34**: 251-262.

**Jongebloed U, Szederkenyi J, Hartig K, Schobert C, Komor E. 2004.** Sequence of morphological and physiological events during natural ageing and senescence of a castor bean leaf: sieve tube occlusion and carbohydrate back-up precede chlorophyll degradation. *Physiologia Plantarum* **120**: 338-346.

**Jump AS, Peñuelas J. 2005.** Running to stand still: adaptation and the response of plants to rapid climate change. *Ecology Letters* **8**: 1010-1020.

**Levitt J. 1972.** *Responses of Plant to Environmental Stress*. N.Y.: Academic Press.

**Loss SP, Siddique KHM. 1994.** Morphological and physiological traits associated with wheat yield increases in Mediterranean environments. *Advances in Agronomy* **52**: 229-276.

**Maggio A, De Pascale S, Fagnano M, Barbieri G. 2011.** Saline agriculture in Mediterranean environments. *Italian Journal of Agronomy* **6**: 36-43.

**Matesanz S, Gianoli E, Valladares F. 2010.** Global change and the evolution of phenotypic plasticity in plants. *Annals of the New York Academy of Sciences* **1206**: 35-55.

**Merzlyak MN, Gitelson AA, Chivkunova OB, Rakitin VY. 1999.** Non-destructive optical detection of pigment changes during leaf senescence and fruit ripening. *Physiologia Plantarum* **106**: 135-141.

**Mickelbart MV, Hasegawa PM, Bailey-Serres J. 2015.** Genetic mechanisms of abiotic stress tolerance that translate to crop yield stability. *Nature Reviews Genetics* **16**: 237-251.

**Miller G, Suzuki N, Ciftci-Yilmaz S, Mittler R. 2010.** Reactive oxygen species homeostasis and signalling during drought and salinity stresses. *Plant Cell and Environment* **33**: 453-467.

**Mittler R. 2017.** ROS are good. *Trends in Plant Sciences* **22**: 11-19.

**Mittler R, Blumwald E. 2010.** Genetic engineering for modern agriculture: challenges and perspectives. *Annual Review of Plant Biology* **61**: 443-462.

**Naschitz S, Naor A, Genish S, Wolf S, Goldschmidt EE. 2010.** Internal management of non-structural carbohydrate resources in apple leaves and branch wood under a broad range of sink and source manipulations. *Tree Physiology* **30**: 715-727.

**Nicotra AB, Atkin OK, Bonser SP, Davidson AM, Finnegan EJ, Mathesius U, Poot P, Purugganan MD, Richards CL, Valladares F, et al. 2010.** Plant phenotypic plasticity in a changing climate. *Trends in Plant Sciences* **15**: 684-692.

**Nilson SE, Assmann SM. 2010.** Heterotrimeric G proteins regulate reproductive trait plasticity in response to water availability. *New Phytologist* **185**: 734-746.

**Nisar N, Li L, Lu S, Khin NC, Pogson BJ. 2015.** Carotenoid metabolism in plants. *Molecular Plant* **8**: 68-82.

**Pigliucci M. 2001.** Phenotypic Plasticity: Beyond Nature and Nurture. Baltimore, MD: The Johns Hopkins University Press.

**Priest HD, Fox SE, Rowley ER, Murray JR, Michael TP, Mockler TC. 2014.** Analysis of global gene expression in *Brachypodium distachyon* reveals extensive network plasticity in response to abiotic stress. *PLoS One* **9**: e87499.

**Reguera M, Peleg Z, Blumwald E. 2012.** Targeting metabolic pathways for genetic engineering abiotic stress-tolerance in crops. *Biochimica et Biophysica Acta* **1819**: 186-194.

**Rontein D, Basset G, Hanson AD. 2002.** Metabolic engineering of osmoprotectant accumulation in plants. *Metabolic Engineering* **4**: 49-56.

**Rosenwasser S, Fluhr R, Joshi JR, Leviatan N, Sela N, Hetzroni A, Friedman H. 2013.** ROSMETER: a bioinformatic tool for the identification of transcriptomic imprints related to

reactive oxygen species type and origin provides new insights into stress responses. *Plant Physiol.* **163**: 1071-1083.

**Rossi M, Bermudez L, Carrari F. 2015.** Crop yield: challenges from a metabolic perspective. *Current Opinion in Plant Biology* **25**: 79-89.

**Rozema J, Flowers T. 2008.** Crops for a salinized world. *Science* **322**: 1478-1480.

**Ruan YL. 2014.** Sucrose metabolism: gateway to diverse carbon use and sugar signaling. *Annual Review of Plant Biology* **65**: 33-67.

**Sade N, Del Mar Rubio-Wilhelmi M, Umnajkitikorn K, Blumwald E. 2018.** Stress-induced senescence and plant tolerance to abiotic stress. *Journal of Experimental Botany* **69**: 845–853.

**Salguero-Gomez R, Jones OR, Jongejans E, Blomberg SP, Hodgson DJ, Mbeau-Ache C, Zuidema PA, de Kroon H, Buckley YM. 2016.** Fast-slow continuum and reproductive strategies structure plant life-history variation worldwide. *Proceedings of the National Academy of Sciences, USA* **113**: 230-235.

**Schlichting CD, Smith H. 2002.** Phenotypic plasticity: linking molecular mechanisms with evolutionary outcomes. *Evolutionary Ecology* **16**: 189-211.

**Shaar-Moshe L, Blumwald E, Peleg Z. 2017.** Unique physiological and transcriptional shifts under combinations of salinity, drought, and heat. *Plant Physiology* **174**: 421-434.

**Shaar-Moshe L, Hubner S, Peleg Z. 2015.** Identification of conserved drought-adaptive genes using a cross-species meta-analysis approach. *BMC Plant Biology* **15**: 111.

**Shabala S, Shabala L. 2011.** Ion transport and osmotic adjustment in plants and bacteria. *Biomolecular Concepts* **2**: 407-419.

**Sultan SE. 2000.** Phenotypic plasticity for plant development, function and life history. *Trends in Plant Sciences* **5**: 537-542.

**Suzuki N, Rivero RM, Shulaev V, Blumwald E, Mittler R. 2014.** Abiotic and biotic stress combinations. *New Phytologist* **203**: 32-43.

**Thalmann M, Pazmino D, Seung D, Horrer D, Nigro A, Meier T, Kolling K, Pfeifhofer HW, Zeeman SC, Santelia D. 2016.** Regulation of leaf starch degradation by abscisic acid is important for osmotic stress tolerance in plants. *Plant Cell* **28**: 1860-1878.

**Thalmann M, Santelia D. 2017.** Starch as a determinant of plant fitness under abiotic stress. *New Phytologist* **214**: 943-951.

**van Kleunen M, Fischer M. 2005.** Constraints on the evolution of adaptive phenotypic plasticity in plants. *New Phytologist* **166**: 49-60.

**Vautard R, Yiou P, D'Andrea F, de Noblet N, Viovy N, Cassou C, Polcher J, Ciais P, Kageyama M, Fan Y. 2007.** Summertime European heat and drought waves induced by wintertime Mediterranean rainfall deficit. *Geophysical Research Letters* **34**.

**Violle C, Navas ML, Vile D, Kazakou E, Fortunel C, Hummel I, Garnier E. 2007.** Let the concept of trait be functional! *Oikos* **116**: 882-892.

**Watt M, Moosavi S, Cunningham SC, Kirkegaard JA, Rebetzke GJ, Richards RA. 2013.** A rapid, controlled-environment seedling root screen for wheat correlates well with rooting depths at vegetative, but not reproductive, stages at two field sites. *Annals of Botany* **112**: 447-455.

**Wen F, Wu XZ, Li TJ, Jia ML, Liu XS, Li P, Zhou XJ, Ji XX, Yue XM. 2017.** Genome-wide survey of heat shock factors and heat shock protein 70s and their regulatory network under abiotic stresses in *Brachypodium distachyon*. *PLoS One* **12**.

**Whan AP, Smith AB, Cavanagh CR, Ral JP, Shaw LM, Howitt CA, Bischof L. 2014.** GrainScan: a low cost, fast method for grain size and colour measurements. *Plant Methods* **10**: 23.

**Xia J, Wishart DS. 2016.** Using MetaboAnalyst 3.0 for comprehensive metabolomics data analysis. *Current Protocols in Bioinformatics* **55**: 14.10.11-14.10.91.

**Yermiyahu U, Heuer B, Silverman D, Faingold I, Avraham L. 2017.** Nitrate analysis of *Diplotaxis tenuifolia*: fresh versus dry material for meeting international standards and regulations. *Israel Journal of Plant Sciences*: 1-4.

**Zandalinas SI, Mittler R, Balfagon D, Arbona V, Gomez-Cadenas A. 2018.** Plant adaptations to the combination of drought and high temperatures. *Physiologia plantarum* **162**: 2-12.

## Supporting Information

Additional Supporting Information may be found online in the Supporting Information tab for this article:

**Fig S1** Germination rate of grains that developed on plants subjected to control conditions and combinations of stresses.

**Fig S2** Association between leaf ROS content and physiological traits or gene expression pattern.

**Fig S3** Association between leaf starch content and physiological traits or gene expression pattern.

**Fig S4** Galactose metabolic pathway under combinations of stresses.

**Fig S5** Potassium / Sodium ratio and chloride concentration in leaves under control and combinations of stresses.

**Fig S6** Climatic conditions in the geographical origin of *Brachypodium distachyon* accession Bd21-3.

**Table S1** Statistical analysis of physiological traits at three developmental stages.

**Table S2** List of differentially expressed genes (DEGs) that were used for correlation analyses.

**Table S3** List of fold change (FC) and false discovery rate (FDR) values of putative metabolites, identified by GC-MS analysis.